Journal of Thermal Science Vol.29, No.5 (2020) 1165−1179

https://doi.org/10.1007/s11630-020-1302-6 **Article ID: 1003-2169(2020)05-1165-15**

Proposal and Assessment of an Engine-Based Distributed Steam and Power Cogeneration System Integrated with an Absorption-Compression Heat Pump

LIU Changchun[1,2,3], HAN Wei[1,2,3*], WANG Zefeng[1,2,3], ZHANG Na[1,2,3]

1. Institute of Engineering Thermophysics, Chinses Academy of Sciences, Beijing 100190, China
2. Beijing Key Laboratory of Distributed Combined Cooling Heating and Power System, Beijing 100190, China
3. University of Chinese Academy of Sciences, Beijing 100049, China

Abstract: Internal combustion engine-based poly-generation systems have been widely used for energy savings and emissions reductions. To maximize their thermodynamic and environmental performance potentials, the efficient recovery of flue gas and jacket water heat is essential. In a conventional internal combustion engine-based steam and power cogeneration system, the low-temperature (less than 170°C) heat from flue gas and jacket water is usually directly discharged to the environment, which dramatically reduces the thermal and economic performance. In this work, a high-temperature heat pump is employed to recover this part of low-temperature heat for steam generation. The sensible heat of the flue gas and jacket water is cascade utilized in a steam generator and a heat pump. Simulation results show that the process steam yield of the proposed system is almost doubled (increased by 703 kg/h) compared to that of an engine-based cogeneration system without a heat pump. The proposed system can reduce natural gas consumption, CO_2 and NO_x emissions by approximately 199 069 m^3, 372.64 tons and 3.02 tons per year, respectively, with a primary energy ratio and exergy efficiency of 72.52% and 46.28%, respectively. Moreover, the proposed system has a lower payback period with a value of 5.11 years, and the determining factors that affect the payback period are natural gas and electricity prices. The total net present value of the proposed system within its lifespan is 2 441 581 USD, and an extra profit of 785 748 USD can be obtained compared to the reference system. This is a promising approach for replacing gas boilers for process steam production in industrial sectors.

Keywords: steam and power cogeneration, HACHP, ICE, high-temperature heat pump

1. Introduction

Currently, industry remains the largest final energy consumption sector, accounting for 37% of total final energy consumption [1], and is the key target for energy conservation and emission reduction. Steam is an important energy carrier and raw material in the chemical [2], food processing [3] and textile industries [4]. It is estimated that steam generation takes up approximately one-third of the overall energy intake in the manufacturing industry [5]. Furthermore, the steam consumed in manufacturing is typically generated by gas boilers, which causes severe environmental problems [6]. Steam and power cogeneration systems not only have promising market prospects but also can simultaneously save energy and reduce emissions. Internal combustion

Received: Apr 09, 2020 Corresponding author: HAN Wei E-mail: hanwei@iet.cn

Abbreviations

ABS	Absorber	REC	rectifier
ANR	annual net revenue/USD	SCR	selective catalytic regeneration
AP	ammonia pump	SP	solution pump
AUX	auxiliary equipment	ST	steam
CIF	cash inflow/USD	*TIV*	total initial investment/ USD
COF	cash outflow/USD	*TNPV*	total net present value/USD
COM	compressor	VAL	valve
CON	condenser	**Symbols**	
ch	chemical	0	environment
ESR	energy saving ratio/%	A	area/m^2
EVA	evaporator	D	destruction
HACHP	hybrid absorption-compression heat pump	E	exergy/kW
HEX	heat exchanger	M	relative molecular mass
HRSG	heat recovery steam generator	N	year/a
ICE	internal combustion engine	Q	thermal energy/kW
JW	jacket water	T	temperature/°C
LHV	low calorific value/kJ·kg^{-1}	W	electricity/kW
MIX	mixer	Z	cost/USD
NG	natural gas	e	specific exergy/kJ·kg^{-1}
NPV	net present value/USD	η_{ex}	exergy efficiency/%
O&M	operation and maintenance	h	specific enthalpy/kJ·kg^{-1}
PBP	payback period/a	i	discount rate
PC	partial condenser	m	mass flow rate/kg·s^{-1}
PER	primary energy ratio/%	n	equipment lifetime
ph	physical	s	specific entropy/kJ·(kg·K)$^{-1}$
REB	reboiler	x	mass concentration/%

engine (ICE)-based poly-generation technologies have received increased attention due to their high efficiency, reliability and modularity [7]. Numerous works on engine-based poly-generation systems have been reported that considering system design, optimization, and operating strategies [8].

For ICE-based ploy-generation systems, the efficient recovery of jacket water heat as well as flue gas heat is essential [9]. Flue gas heat, which has a higher temperature up to 450°C, can be used to produce steam or drive refrigerants for cooling [10]. Aly et al. [11] evaluated an engine-based diffusion absorption refrigerator for cooling and verified with experimental data. The result indicated that a maximum waste heat recovery of 10% can be obtained. The heat from the jacket water, with a temperature range from 70°C to 100°C, is mostly employed to produce domestic hot water [12]. Yang et al. [13] proposed an ICE-based dual-fuel tri-generation system and revealed its thermodynamic and exergoeconomic performance. The jacket water heat in the proposed system is recovered by a plate heat exchanger to produce hot water for a hypothetical hotel. Javan et al. [14] analyzed an ICE-based tri-generation system for residential applications with various types of working fluids. The results indicated that R11 working fluid is a highly suitable choice in terms of both thermodynamics and economic performance. Yan et al. [15] investigated a tri-generation system for a cruise ship based on multi-objective optimization, noting that CO, NO_x and SO_x emissions reductions of up to 61.3% could be obtained. Pérez et al. [16] discussed an ICE-based cogeneration system to be installed in isolated communities from the perspective of economic and energetic analyses, and noted that the unit electricity cost was 0.022 USD/kWh with a payback period (*PBP*) of 5.3 years. Segurado et al. [17] reviewed biomass-associated tri-generation systems from the perspective of techno-economic analysis. The results showed that an increase in the natural gas cost or a decline in the biomass cost could render this type of system financially feasible. Researchers have also considered using a

Rankine cycle as the bottoming cycle to recover low-temperature heat for power generation [18]. However, the high initial investment is the main barrier to the diffusion of this technology.

Most ICE-based poly-generation systems have been developed for hotels, office buildings, data centers and residential buildings because these consumers possess hot water and/or cooling demand [19]. For industrial sectors, however, low-grade jacket water heat, which accounts for up to 30% of the entire system energy input, is usually directly discharged to the environment as waste heat because it cannot be employed to produce steam or electricity that is beneficial to the industry. The low-temperature waste heat is able to be retrieved and upgraded by a high-temperature heat pump [20]. Urbanucci et al. [21] evaluated the thermodynamic and economic potential of integrating high-temperature heat pumps into tri-generation systems. The results indicated that heat pump-enhanced systems can provide a cost savings up to 40%. To date, there is no heat pump used for steam generation that recovers low-temperature waste heat for commercial applications due to the restrictions of high-temperature and high-pressure ratio compressors [22]. A hybrid absorption-compression heat pump (HACHP), which adopts commercially established technologies (low-pressure ratio compressors, pumps and heat exchangers), is a promising steam production approach by recovering low-temperature heat [23].

In this work, a high-temperature heat pump enhanced steam and power cogeneration system is developed. In contrast to conventional ICE-based cogeneration systems, the low-temperature heat remained in the flue gas and the jacket water is utilized in cascades to generate high-quality process steam rather than discharged as waste or to produce low-quality hot water. As a result, the process steam producing gas boiler, which has high energy consumption and high pollution production, can be removed. The thermodynamic performance of this proposed steam and power cogeneration system is analyzed in comparison with that of a conventional ICE-based cogeneration system. Meanwhile, the emissions reduction potential of the proposed system is revealed. Then, the irreversible losses and the performance improvement mechanism of the proposed system are identified via an exergy analysis. Finally, a parameter analysis of the produced process steam pressure and an economic analysis are carried out to reveal the application potential of the proposed cogeneration system.

2. System Description

The proposed cogeneration system mainly consists of an ICE, an HRSG, an HACHP and a selective catalytic regeneration (SCR) denitration subsystem, as described in Fig. 1. The ICE acts as the prime mover to generate electrical power, while the HRSG and the HACHP subsystem serves as bottom cycle to reclaim the jacket water and flue gas heat for process steam generation. The HACHP subsystem refers to a high-temperature heat pump that originates from a typical ACHP system and can dramatically cut down the power consumption and

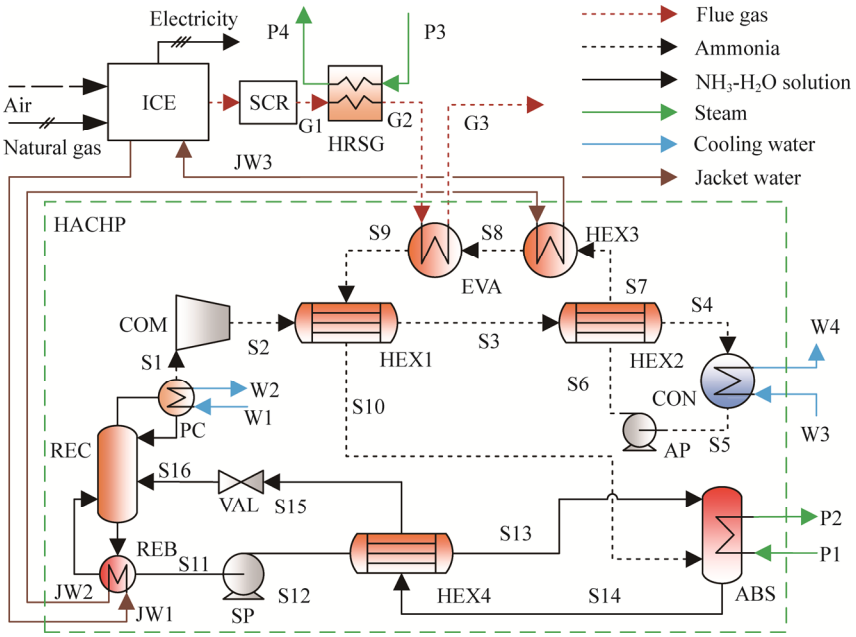

Fig. 1 Sketch of the proposed cogeneration system

reduce compressor discharge temperature [23]. The ammonia-rich vapor (S1) from the rectifier (REC) is first compressed into a mid-pressure (which is determined by ambient temperature) ammonia-rich vapor (S2) by the compressor (COM), then chilled into a liquid by heat exchanger #1 (HEX1), heat exchanger #2 (HEX2) and a condenser (CON) in sequence. Then, the mid-pressure ammonia liquid (S5) is pumped into a high-pressure (which is determined by steam output temperature) ammonia liquid (S6) by an ammonia pump (AP). After that, it is heated into a superheat state (S10) by the HEX2, HEX3, EVA and HEX1 in sequence. Therefore, the power consumption is lower due to the low-pressure ratio for gas compression, along with the compressor discharge temperature decrease. The low-pressure diluted ammonia-water solution (S11) from the REC is pumped and preheated into a high-pressure ammonia-water solution (S13) by a solution pump (SP) and HEX4, respectively. Then, the ammonia-rich vapor (S10) is absorbed by the diluted ammonia-water solution (S13) resulting in a strong ammonia-water solution (S14) in the ABS, accompanying substantial high-temperature heat-releasing; this heat is used to generate high-temperature process steam. Notably, the mid-pressure in the HACHP is determined by ambient temperature. The ammonia-rich vapor from the rectifier is compressed into a pressure that can be condensed into a liquid at ambient temperature. The high-pressure is determined by steam output temperature, and correspondingly the pressures of S6 to S15 are determined. The low-pressure is determined by heat source temperature, which is the temperature of the jacket water and flue gas in this paper. The main purpose of this article is to study the performance of proposed cogeneration system rather than the heat pump itself. A detailed introduction of the HACHP can be found in the previous work of the authors [23]. The jacket water flows by the REC and the HEX3 in sequence to cascade utilize its remained heat. Similarly, the flue gas is introduced into the HRSG and EVA in order according to the cascade utilization of thermal energy. The process steam generated in the HRSG and the ABS is the same temperature.

The reference system of this paper consists of a gas boiler and a conventional ICE-based cogeneration (steam and power) subsystem without the HACHP. The remained heat of the flue gas is recovered by a heat recovery steam generator (HRSG) to produce process steam. Therefore, the process steam in the reference system is provided by both the gas boiler and HRSG. The low-grade jacket water heat, which accounts for up to 30% of the entire system energy input, is directly discharged to the environment as waste heat because it cannot be employed to produce steam or electricity that is beneficial to the industry in this system.

3. Simulation and Assumptions

In this section, mathematical models and evaluation criteria for evaluating the thermal and economic performance of the proposed cogeneration system are developed. Then, general assumptions and parameters are specified for the simulation.

3.1 Energy analysis model

For thermodynamic analysis, each component of the proposed cogeneration system is regarded as a control volume with solution paths, work interactions and heat transfer. The mass, component and energy balance of each control volume are described as follow:

$$\sum_{\text{in}} m_{\text{in}} - \sum_{\text{out}} m_{\text{out}} = 0 \tag{1}$$

$$\sum_{\text{in}} m_{\text{in}} x_{\text{in}} - \sum_{\text{in}} m_{\text{out}} x_{\text{out}} = 0 \tag{2}$$

$$\sum_{\text{in}} m_{\text{in}} h_{\text{in}} - \sum_{\text{out}} m_{\text{out}} h_{\text{out}} + W + Q = 0 \tag{3}$$

where m, x and h are the mass flow rate, the ammonia mass fraction and the specific enthalpy of the solution, respectively. W and Q denote the work interaction and heat transfer of the control volume, respectively. The subscripts in and out refer to the entrance and exit of the control volume, respectively. The energy balance equation of each component in the proposed system is presented in Table 1.

Table 1 Energy balance equation of each component

Items	Energy balance equation
ICE	$m_{NG}\cdot LHV_{NG}+m_{JW3}\cdot h_{JW3}+m_{air}\cdot h_{air}=W_{ICE}+m_{G1}\cdot h_{G1}+m_{JW1}\cdot h_{JW1}$
HRSG	$m_{G1}\cdot h_{G1}=Q_{HRSG}+m_{G2}\cdot h_{G2}$
REC	$m_{S16}\cdot h_{S16}+Q_{REB}=Q_{PC}+m_{S1}\cdot h_{S1}+m_{S11}\cdot h_{S11}$
COM	$m_{S1}\cdot h_{S1}+W_{COM}=m_{S2}\cdot h_{S2}$
HEX1	$m_{S2}\cdot h_{S2}+m_{S9}\cdot h_{S9}=m_{S3}\cdot h_{S3}+m_{S10}\cdot h_{S10}$
HEX2	$m_{S3}\cdot h_{S3}+m_{S6}\cdot h_{S6}=m_{S4}\cdot h_{S4}+m_{S7}\cdot h_{S7}$
HEX3	$m_{S7}\cdot h_{S7}+m_{JW2}\cdot h_{JW2}=m_{S8}\cdot h_{S8}+m_{JW3}\cdot h_{JW3}$
EVA	$m_{G2}\cdot h_{G2}=Q_{EVA}+m_{G3}\cdot h_{G3}$
CON	$m_{S4}\cdot h_{S4}=Q_{CON}+m_{S5}\cdot h_{S5}$
AP	$m_{S5}\cdot h_{S5}+W_{AP}=m_{S6}\cdot h_{S6}$
SP	$m_{S11}\cdot h_{S11}+W_{SP}=m_{S12}\cdot h_{S12}$
HEX4	$m_{S12}\cdot h_{S12}+m_{S14}\cdot h_{S14}=m_{S13}\cdot h_{S13}+m_{S15}\cdot h_{S15}$
ABS	$m_{S10}\cdot h_{S10}+m_{S13}\cdot h_{S13}=Q_{ABS}+m_{S14}\cdot h_{S14}$

Based on the first law of thermodynamics, two parameters (the primary energy ratio, *PER*, and the primary energy saving ratio, *ESR*) are employed to evaluate the thermodynamic performance of the proposed cogeneration system. The *PER* is the ratio of the energy export to the primary energy intake of the proposed

cogeneration system, which corresponds to the degree of primary energy utilization.

$$PER=\frac{W_{\text{output}}+Q_{\text{HRSG}}+Q_{\text{HACHP}}}{Q_{\text{NG}}} \tag{4}$$

where Q_{NG} refers to the thermal energy intake of the system from natural gas, while Q_{HRSG} and Q_{HACHP} refer to the heat output from the HRSG and HAHCP, respectively. W_{output} represents the electrical power output of the proposed cogeneration system.

The *ESR* is the ratio of the decrease in energy intake of the proposed cogeneration system compared to that of conventional separate generation systems for the same amounts of electrical power and process steam output:

$$ESR=1-\frac{Q_{\text{NG}}}{Q_{\text{S,in}}}=1-\frac{Q_{\text{NG}}}{\frac{W_{\text{output}}}{\eta_{\text{grid}}}+\frac{Q_{\text{HRSG}}}{\eta_{\text{b}}}+\frac{Q_{\text{HACHP}}}{\eta_{\text{b}}}} \tag{5}$$

where $Q_{\text{S,in}}$ refers to the natural gas energy intake of the separate production system. η_{grid} and η_{b} represent the efficiency of the grid and gas boiler, respectively.

3.2 Exergy analysis model

The exergy analysis model is developed to reveal the irreversible losses and the performance improvement mechanism of the proposed cogeneration system. The exergy balance equation of a control volume can be described as:

$$\sum_{i=1}^{n}E_i+\sum_{\text{in}}m_{\text{in}}e_{\text{in}}=\sum_{\text{out}}m_{\text{out}}e_{\text{out}}+W+E_{\text{D}} \tag{6}$$

where E_i, W and E_{D} represent the exergy of the heat flow, the work interaction and the exergy destruction, respectively. m and e refer to the mass flow rate and specific exergy of the solution flow, respectively. The exergy losses and destruction equation of each component is listed in Table 2.

The specific exergy (e) of solution in this paper is considered as the sum of the chemical and physical exergy regardless of the kinetic and potential exergy.

$$e=e_{\text{ch}}+e_{\text{ph}} \tag{7}$$

The chemical exergy calculation formula for the ammonia-water solution is described as follows [24]:

$$e_{\text{ch}}=\frac{x}{M_{\text{NH}_3}}\cdot e^0_{\text{ch,NH}_3}+\frac{1-x}{M_{\text{H}_2\text{O}}}\cdot e^0_{\text{ch,H}_2\text{O}} \tag{8}$$

where $e^0_{\text{ch,H}_2\text{O}}$ and $e^0_{\text{ch,NH}_3}$ represent the chemical exergy of water and ammonia at standard conditions [25], respectively.

The physical exergy is defined as a formula related to the physical states of a solution:

$$e_{\text{ph}}=(h-h_0)-T_0(s-s_0) \tag{9}$$

where T_0, s_0 and h_0 refer to the temperature, specific entropy and enthalpy in the dead state (at ambient temperature and pressure); h and s represent the specific entropy and enthalpy of the ammonia-water solution at the actual working state, respectively.

Table 2 Exergy losses and destruction in each component

Items	Exergy losses and destruction
ICE	$E_{\text{D,ICE}}=E_{\text{NG}}+E_{\text{JW3}}-E_{\text{JW1}}-E_{\text{G1}}-W_{\text{ICE}}$
HRSG	$E_{\text{D,HRSG}}=E_{\text{G1}}+E_{\text{P3}}-E_{\text{G2}}-E_{\text{P4}}$
REC	$E_{\text{D,REC}}=E_{\text{JW1}}+E_{\text{S16}}-E_{\text{JW2}}-E_{\text{S1}}-E_{\text{S11}}$
COM	$E_{\text{D,COM}}=E_{\text{S1}}+W_{\text{COM}}-E_{\text{S2}}$
HEX1	$E_{\text{D,HEX1}}=E_{\text{S2}}+E_{\text{S9}}-E_{\text{S3}}-E_{\text{S10}}$
HEX2	$E_{\text{D,HEX2}}=E_{\text{S3}}+E_{\text{S6}}-E_{\text{S4}}-E_{\text{S7}}$
HEX3	$E_{\text{D,HEX3}}=E_{\text{S7}}+E_{\text{JW2}}-E_{\text{S8}}-E_{\text{JW3}}$
EVA	$E_{\text{D,EVA}}=E_{\text{S8}}+E_{\text{G2}}-E_{\text{S9}}-E_{\text{G3}}$
CON	$E_{\text{D,CON}}=E_{\text{S4}}-E_{\text{S5}}$
AP	$E_{\text{D,AP}}=E_{\text{S5}}+E_{\text{AP}}-E_{\text{S6}}$
SP	$E_{\text{D,SP}}=E_{\text{S11}}+W_{\text{SP}}-E_{12}$
HEX4	$E_{\text{D,HEX4}}=E_{\text{S12}}+E_{\text{S14}}-E_{\text{S13}}-E_{\text{S15}}$
ABS	$E_{\text{D,ABS}}=E_{\text{S10}}+E_{\text{S13}}-E_{\text{P1}}-E_{\text{S14}}-E_{\text{P2}}$
VAL	$E_{\text{D,VAL}}=E_{\text{S15}}-E_{\text{S16}}$

The ratio of the sum exergy export of the ICE, HRSG and HACHP to the exergy input of the ICE by natural gas is defined as the exergy efficiency and it can be calculated by:

$$\eta_{\text{ex}}=\frac{W+E_{\text{ST}}}{m_{\text{f}}\cdot e_{\text{f}}} \tag{10}$$

where W and E_{ST} are the output power and the steam exergy, respectively, m_{f} is the fuel mass flow, and e_{f} is the fuel specific exergy [26].

$$e_{\text{f}}=LHV_{\text{f}}\cdot\left(1.033+0.0169\cdot\frac{b}{a}-\frac{0.0698}{a}\right) \tag{11}$$

where a and b are constants related to the fuel composition. LHV_{f} is the low heating value of fuel.

3.3 Economic analysis model

To assess the economic performance of this proposed cogeneration system, the costs of the key components are obtained from previous open published studies. The initial investment of the ICE is given by [27]:

$$Z_{\text{ICE}}=-138.71\cdot\ln(W_{\text{ICE}})+1727.1 \tag{12}$$

The initial investment of the HRSG [28]:

$$Z_{\text{HRSG}}=4745\cdot\left(\frac{h_{\text{ST}}}{\log(T_{\text{i}}-T_0)}\right)^{0.8}+11820\cdot m_{\text{ST}}+658\cdot m_{\text{G}} \tag{13}$$

where h_{ST} is the enthalpy transferred to steam, kW. m_{ST} and m_{G} represent the mass flow rate of the steam and flue gas, respectively.

The initial investment of the compressor [29]:

$$Z_{\mathrm{COM}}=9624.2\cdot W_{\mathrm{COM}}^{0.46} \tag{14}$$

The initial investment of the pumps [30]:

$$Z_{\mathrm{pump}}=3540\cdot W_{\mathrm{pump}}^{0.71} \tag{15}$$

The cost of heat exchangers, including the HEX1, HEX2, HEX3, HEX4, CON, EVA, ABS and REC, are determined by its heat exchange area using the power law [31]:

$$Z_{\mathrm{k}}=Z_{R,k}\cdot\left(\frac{A_k}{A_R}\right)^{0.6} \tag{16}$$

where $Z_{R,k}$ and A_R are the reference cost and area, respectively, and the reference cost of each component with a heat exchange area of 100 m^2 is presented in Table 3 [31].

Table 3 Reference costs of heat exchangers with an area of 100 m^2

Items	Reference cost/USD
HEX4	12 000
ABS	16 500
REC	17 000
EVA, HEX1, HEX2, HEX3, CON	16 000

Except for the costs of the aforementioned key components, the costs of auxiliary equipment (AUX) such as pipeline and control systems are also an important part of the overall initial investment. The cost of the AUX normally accounts for 10% to 15% that of the key components [32, 33], which is set as 12% in this paper. The total initial investment (*TIV*) can be calculated by:

$$TIV=Z_{\mathrm{ICE}}+Z_{\mathrm{HRSG}}+Z_{\mathrm{HACHP}}+Z_{\mathrm{AUX}} \tag{17}$$

where Z_{HACHP} refers to the initial investment of the HACHP, including the costs of the pumps, heat exchangers and compressor.

The annual net revenue (*ANR*) after the plant is built can be calculated by:

$$ANR=CIF_{\mathrm{electricity}}+CIF_{\mathrm{steam}}-COF_{\mathrm{NG}}-COF_{\mathrm{O\&M}} \tag{18}$$

where *CIF* and *COF* represent cash inflow and cash outflow, respectively. Moreover, the operation and maintenance (O&M) cost at each year is set to 4% of the overall initial investment [34].

The net present value (*NPV*) is the *ANR* considering the time value of money.

$$NPV_n=\frac{ANR}{(1+i)^n} \tag{19}$$

where *i* represents the discount rate [35]. Notably, NPV_0 refers to the total initial investment.

The total net present value (*TNPV*) in this paper is defined as:

$$TNPV_n=\sum_0^n NPV_n \tag{20}$$

The *PBP* is given by:

$$PBP=N-1+\frac{\left|\sum_0^{n-1}NPV_n\right|}{NPV_n} \tag{21}$$

where *N* refers to the year when the *TNPV* is positive.

3.4 Assumption and parameter specification

To assess the thermodynamic performance of the proposed cogeneration system, a Caterpillar internal combustion engine (CAT G3512E) with a capacity of 1200 kW is adopted as the prime mover; its key parameters are summarized in Table 4. The model of ICE that was proposed by Sanaye et al. [36] is used to calculate the engine characteristics at various operating conditions, which has been demonstrated to be consistent with the experimental data of an ICE of type CAT G3512E [37]. Additional simulation parameters, including the parameters for economic and environmental analysis, are presented in Table 5 [38, 39]. The proposed cogeneration system is modelled employing the Engineering Equation Solver (EES) [40].

Table 4 Main parameter of the ICE CAT G3512E

Item	Value	Item	Value
No. of cylinders	12	Compression ratio	11.9
Rated power/kW	1200	Exhaust flow/L	52
Engine speed/r·min^{-1}	1500	Rated efficiency/%	42

Table 5 Additional parameters for the simulation

Items	Value
Ambient temperature/°C	25
Efficiency of the gas boiler/%	90
Efficiency of the grid/%	35
LHV of natural gas/kJ·m^{-3}	36 620
Ammonia mass fraction in strong solution/%	33
Natural gas CO_2 emission factor/g·kWh^{-1}	184
Natural gas NO_x emission factor/g·kWh^{-1}	1.49
Plant lifespan/a	20
Natural gas price/USD·m^{-3}	0.35
Electricity price/USD·kWh^{-1}	0.12
Steam price/USD·kg^{-1}	0.013
Nominal interest ratio/%	7
Inflation rate/%	2

4. Results and Discussion

The thermodynamic and environmental performance of this proposed cogeneration system in the basic case is revealed via an energy analysis in Section 4.1. Then, the performance improvement mechanism of this proposed cogeneration system is revealed via exergy analysis in

Section 4.2. Furthermore, to assess the application potential of the proposed cogeneration system, an economic analysis is conducted in Section 4.3.

4.1 Thermodynamic performance comparison

The flow properties at different state points in Fig. 1 are summarized in Table 6. The high-temperature (above 171.84°C) flue gas heat is directly transported to the process steam through the HRSG, while the low-temperature (below 171.84°C) heat is recovered by the evaporator of the HACHP subsystem. The temperature of flue gas discharged to the environment, which is usually as high as 170°C for a conventional ICE-based CHP system without the HACHP, decreases to 91.02°C in the proposed cogeneration system. Similarly, the jacket water with a higher temperature (from 90°C to 83.13°C) acts as the heat source of the reboiler in the HACHP subsystem, while its low-temperature (from 83.13°C to 79.87°C) heat is utilized to preheat the ammonia solution in HEX3. The process steam

Table 6 Flow properties at different state points in Fig. 1

Item	T /°C	p /MPa	m /kg·h^{-1}	h /kJ·kg^{-1}	s /kJ·(kg·K)$^{-1}$	E /kW
S1	64.15	0.34	1500	–3122	–5.94	75.48
S2	190.00	1.16	1500	–2844	–5.81	175.98
S3	131.52	1.16	1500	–2990	–6.15	157.13
S4	47.69	1.16	1500	–3431	–7.40	128.62
S5	31.34	1.16	1500	–4486	–10.83	115.51
S6	32.10	3.45	1500	–4481	–10.83	117.07
S7	75.10	3.45	1500	–4040	–9.52	138.31
S8	81.02	3.45	1500	–3557	–8.14	168.24
S9	116.52	3.45	1500	–3169	–7.09	199.01
S10	142.98	3.45	1500	–3024	–6.72	214.34
S11	79.68	0.34	8500	–13 170	–8.86	47.21
S12	80.14	3.45	8500	–13 166	–8.86	55.87
S13	151.80	3.45	8500	–12 835	–8.00	237.55
S14	156.80	3.45	10 000	–11 527	–8.17	312.52
S15	99.17	3.45	10 000	–11 808	–8.87	112.32
S16	68.52	0.34	10 000	–11 808	–8.84	82.26
G1	434.08	0.10	6511	–1793	1.01	334.65
G2	171.84	0.10	6511	–2095	0.48	75.78
G3	91.02	0.10	6511	–2184	0.25	33.58
JW1	90.00	0.10	53 082	–15 594	–8.24	382.36
JW2	83.13	0.10	53 082	–15 623	–8.32	309.64
JW3	79.87	0.10	53 082	–15 637	–8.35	277.58
P1	100.00	0.50	703	–15 552	–8.12	6.71
P2	152.16	0.50	703	–13 224	–2.61	140.40
P3	100.00	0.50	844	–15 552	–8.12	8.05
P4	151.83	0.50	844	–13 224	–2.61	168.46

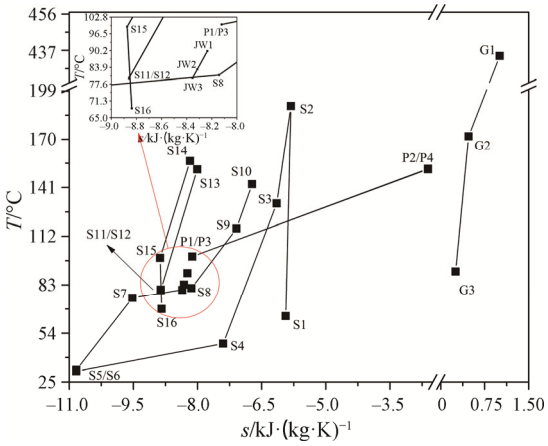

Fig. 2 *T-s* diagram of the proposed system

production is increased by 703 kg/h via the heat recovery of the flue gas and jacket water. A *T-s* diagram is shown in Fig. 2 to present the proposed system more intuitively.

The energy balance and thermodynamic performances of the investigated systems are listed in Table 7. With an intake natural gas flow rate of 280.88 m^3/h, the proposed cogeneration system can simultaneously produce 1071.84 kW of electrical power and 1000.18 kW of process steam at 0.5 MPa. The reference system of this paper consists of a gas boiler, a conventional ICE-based steam and power cogeneration subsystem without the HACHP. To produce the same amounts of products, a natural gas consumption of 309.32 m^3/h is required for the reference cogeneration system, including the natural gas intake of the ICE-based cogeneration subsystem with a value of 250.35 m^3/h and that of the gas boiler with a value of 58.96 m^3/h. For the same amount of net electricity output, the natural gas consumed by the ICE in the proposed system is slightly higher (with a value of 30.53 m^3/h) than that of the ICE in the reference cogeneration system due to the power consumption of the HACHP, which enables the proposed system to produce more steam (703 kg/h). To produce the same amount of process steam, extra natural gas with a value of 58.96 m^3/h, which is consumed by the gas boiler, is needed for the reference cogeneration system. In total, there is a natural gas savings potential of up to 199 069 m^3 per year, considering an annual operating time of 7000 hours.

The total heat loss in this proposed cogeneration system is 785.12 kW, and approximately 26.93% of the heat loss is avoided compared to the reference cogeneration system. More specifically, the amount of heat discharged to the environment by the ICE flue gas is reduced by 50%; all heat extracted from ICE by jacket water is recovered by the HACHP, and a heat loss of 59.98 kW caused by the gas boiler flue gas is avoided. There is an increased heat loss with a value of 4310.13 kW for the proposed system, which is removed by the

Table 7 Thermodynamic performance of the investigated systems

Item	Proposed system	Reference system		
	ICE-HRSG-HACHP	Sum	ICE-HRSG	Gas boiler
Natural gas intake				
Volume flow rate/$m^3 \cdot h^{-1}$	280.88	309.32	250.35	58.96
Energy input/kW	2857.14	3146.46	2546.66	599.80
Net electricity output/kW	1071.84	1071.84	1071.84	–
Electricity generation/kW	1200	1071.84	1071.84	–
HACHP consumption/kW	–128.16	–	–	–
Steam generation				
Steam heat output/kW	1000.18	1000.18	460.36	539.82
Steam flow rate/$kg \cdot h^{-1}$	1546.80	1546.80	711.96	834.84
Heat loss/kW	785.12	1074.44	1014.46	59.98
Flue gas/kW	123.71	290.16	230.18	59.98
Jacket water/kW	–	569.71	569.71	–
Cooling water/kW	439.72	–	–	–
Other loss/kW	221.69	211.35	211.35	–
PER/%	72.52		65.85	
ESR/%	22.01		14.11	

cooling water of the condenser in the HACHP. The remaining heat loss, which mainly occurs in the ICE, in the proposed system (221.69 kW) is slightly higher than that in the reference cogeneration system (211.35 kW) due to the higher operating load. Finally, the *PER* and the *ESR* of the proposed system reach 72.52% and 22.01%, which are increased by 10.13% and 55.98% compared to those of the reference cogeneration system, respectively.

The emissions of the proposed and reference cogeneration systems are calculated using the CO_2 and NO_x emission factors of the natural gas, as presented in Fig. 3, including the CO_2 and NO_x emission rates. The CO_2 emission rate in the proposed cogeneration system is approximately 525.71 kg/h, which is decreased by 9.19% compared to the reference cogeneration system. The NO_x emission rates of the proposed cogeneration system and reference cogeneration system are approximately 4.26 kg/h and 4.69 kg/h, respectively. Hence, the proposed cogeneration system would reduce CO_2 and NO_x emissions by approximately 372.64 tons and 3.02 tons per year, respectively, compared to the reference cogeneration system.

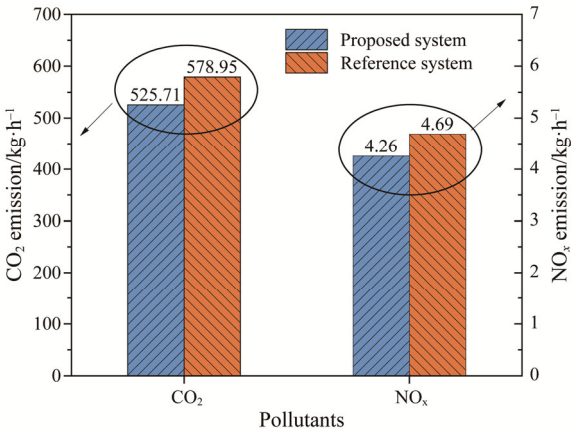

Fig. 3 Emission reduction performance of the proposed cogeneration system

4.2 Performance improvement mechanism

An exergy analysis is conducted to assess the performance improvement mechanism of the proposed cogeneration system. With an exergy intake of 2951.26 kW, the exergy balance results of this proposed cogeneration system are presented in Fig. 4. The exergy outputs, in the forms of steam and electricity, are 294.09 kW (9.96%) and 1071.84 kW (36.32%), respectively. The results show that the exergy destruction is mainly distributed at the ICE, which takes 44.45% of the total fuel exergy (2951.26 kW) input. This is due to the considerable chemical exergy destruction of the combustion process. The exergy destructions of the HRSG and the flue gas are 98.47 kW (3.34%) and 33.58 kW (1.14%), respectively. Furthermore, the total exergy destruction in the HACHP is 141.45 kW (4.79%), while the exergy destruction at each component of the HACHP subsystem is no more than 1.2%; hence, the exergy of the jacket water and the HRSG flue gas are well utilized.

The comparison results of the investigated systems under exergy analysis are summarized in Table 8. For the same amount of product generation, the exergy demand

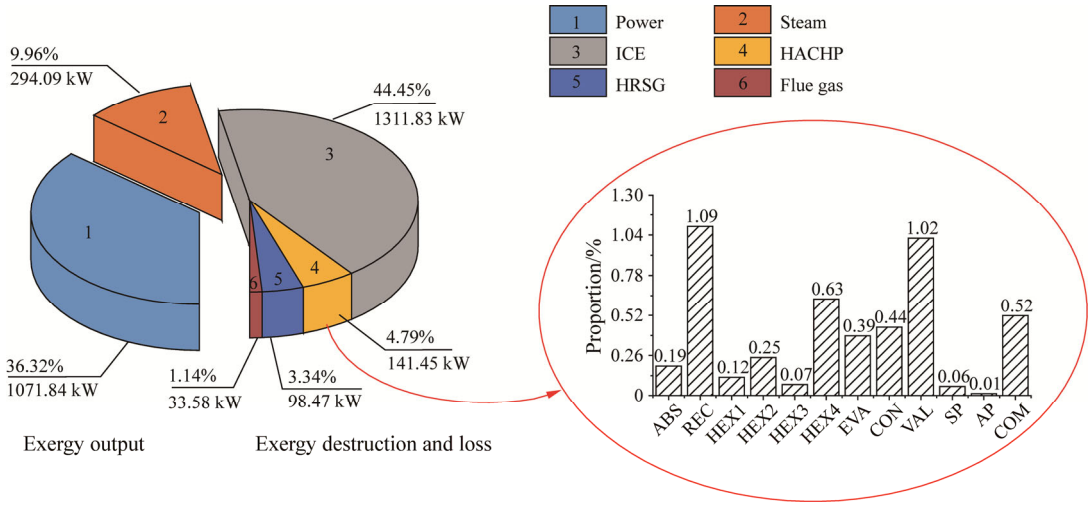

Fig. 4 Exergy balance of the proposed cogeneration system

Table 8 Comparison of the investigated systems under exergy analysis

Item	Proposed cogeneration system		Reference cogeneration system	
	Value/kW	Ratio/%	Value/kW	Ratio/%
Exergy input	2951.26	100	3250.10	100
ICE	2951.26	100	2630.55	80.94
Gas boiler	–	–	619.55	19.06
Exergy destruction	1547.69	52.44	1625.65	50.02
Combustion process	1311.83	44.45	1338.02	41.17
ICE	1311.83	44.45	1169.26	35.98
Gas boiler	–	–	168.76	5.19
Heat transfer process	150.39	5.10	287.63	8.85
HRSG	98.47	3.34	87.77	2.70
Heat exchangers	42.87	1.45	–	–
CON	9.05	0.31	–	–
Gas boiler	–	–	199.86	6.15
Pressure change process	47.49	1.61	–	–
Absorption and desorption process	37.98	1.29	–	–
Exergy loss	37.64	1.28	260.30	8.01
Flue gas	33.58	1.14	83.45	2.57
ICE	33.58	1.14	67.55	2.08
Gas boiler	–	–	15.91	0.49
Jacket water	–	–	93.39	2.87
Cooling water	4.06	0.14	–	–
Exergy output	1365.93	46.28	1364.15	41.97
Electricity	1071.84	36.32	1070.06	32.92
Steam	294.09	9.96	294.09	9.05
HRSG	160.43	5.44	143.00	4.40
HACHP	133.66	4.53	–	–
Gas boiler	–	–	151.10	4.65
Exergy efficiency/%	46.28		41.97	

for the reference cogeneration system is 3250.10 kW, including the exergy intake of the ICE with a value of 2630.55 kW and the exergy consumption of the gas boiler with a value of 619.55 kW. The exergy destructions of this proposed cogeneration system and reference cogeneration system are 1547.69 kW and 1625.65 kW, respectively. The exergy destruction occurs during the combustion process and the heat transfer process for both investigated systems, and the extra exergy destruction takes place during the pressure change process, the absorption and desorption process for this proposed cogeneration system. The exergy destructions in the combustion process of the proposed cogeneration system is 1311.83 kW, which is decreased by 1.96% compared to that of the reference cogeneration system. This result can be attributed to the absence of the gas boiler, which causes an exergy destruction of 168.76 kW during the combustion process for the reference cogeneration system. The exergy destructions that occur in the heat transfer process of the proposed system (150.39 kW) decreased by 47.71% compared to the reference cogeneration system (287.63 kW). Although the heat exchangers (HEX1, HEX2, HEX3, HEX4 and EVA) and CON in the proposed cogeneration system bring an additional exergy destruction of 42.87 kW, 199.86 kW of exergy destruction is avoided due to the absence of the gas boiler. The exergy destructions in the pressure change (in the COM, AP, SP and VAL), absorption and desorption processes are 47.49 kW (1.61%) and 37.98 kW (1.29%), respectively. Compared to the reference cogeneration system, the exergy discharged to the environment is dramatically decreased from 260.30 kW to 37.64 kW due to the heat recovery of the jacket water and flue gas. The exergy removed by the flue gas is reduced by 59.77% due to the heat recovery of the flue gas and the absence of the gas boiler. Moreover, an exergy loss with a value of 93.39 kW (2.87%) is avoided because of the heat recovery of the jacket water. In contrast, the exergy loss caused by cooling water in the proposed system with a value of 4.06 kW (0.14%) is negligible. Finally, the exergy efficiency obtained by this proposed cogeneration system reaches 46.28%, which is 10.27% higher than that obtained by the reference cogeneration system.

To gain a more intuitive perspective on the exergy distribution at each part of this proposed cogeneration system and to determine the potential for further performance improvements, the exergy efficiency of each component in the proposed cogeneration system is presented in Fig. 5. The ICE shows the lowest value, followed by the HRSG, and the exergy efficiencies of all these components are below 70%. More attention should be focused on the ICE and the HRSG for further performance improvement of the proposed system.

4.3 Application potential

The performances of the proposed cogeneration system for the generation of process steam at various pressures are presented in Fig. 6. As the produced steam pressure increases from 0.2 MPa to 0.6 MPa, the steam heat output decreases from 1050.38 kW to 977.68 kW

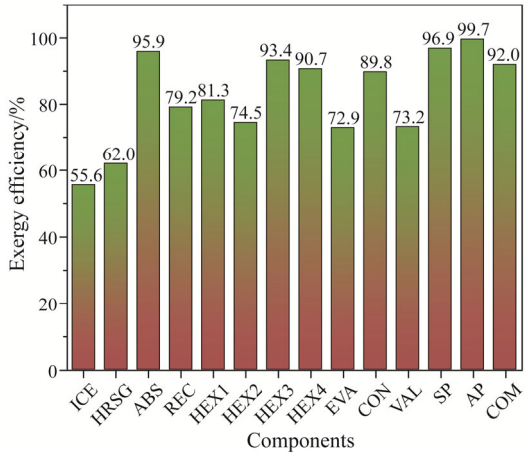

Fig. 5 Exergy efficiency of each component in the proposed cogeneration system

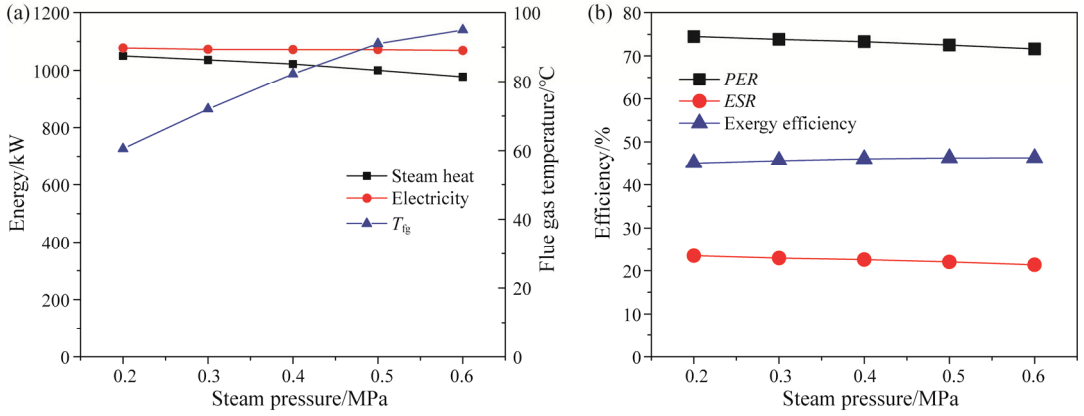

Fig. 6 Effects of produced process steam pressure

because of the increase in the discharged flue gas temperature for high-pressure steam production. The electricity output of the proposed system shows only a small decrease with the steam pressure varying from 0.2 MPa to 0.6 MPa. This slight decrease comes from the increased electricity consumption of the HACHP. A higher absorption pressure, which causes more electricity consumption for the pumps (the AP and SP), is required for higher pressure steam production. An increase in the absorption pressure is realized with liquid compression, so there is only a slight increase in the electrical power intake in the HACHP. With the increase in the produced steam pressure, both the *PER* and the *ESR* decrease. The *PER* decreases from 74.47% to 71.64%, and the *ESR* decreases from 23.34% to 21.34% when the produced steam pressure rises from 0.2 MPa to 0.6 MPa. This result occurs because the temperature of the flue gas discharged into the environment rises with the increase in the steam pressure, and more heat is lost to the environment correspondingly. Interestingly, the exergy efficiency of the proposed system shows a slight increase, varying from 45.09% to 46.31%, with the increase in the steam pressure. The exergy output of the proposed system increases from 1330.74 kW to 1367 kW regardless of the decrease in both the heat and electricity output. The exergy output increase mainly comes from the increased steam quality, which increases the steam exergy output by 17%. As the produced process steam pressure varies from 0.2 MPa to 0.6 MPa, variations in the *PER*, the *ESR* and exergy efficiency are less than three percentage points, and the proposed system is suitable for electricity and steam cogeneration.

To assess the application potential of the proposed cogeneration system, the economic analysis results of the investigated systems are summarized in Table 9. To recover the low-temperature heat remained in the HRSG flue gas and the jacket water, an additional initial investment of 104 979 USD in the HACHP is required. Meanwhile, the initial investment of the gas boiler with a value of 51 856 USD can be avoided. The total initial investment required for the proposed cogeneration system increases by 4.70% compared with that of the reference cogeneration system after considering their AUXs. This proposed cogeneration system has a higher O&M cost than the reference cogeneration system, with a value of 6375 USD. This higher cost occurs because the proposed cogeneration system is relatively complex and has a higher initial investment compared to the reference cogeneration system. The annual fuel cost in this proposed cogeneration system is 688 149 USD, and the annual cost savings on fuel in the proposed cogeneration system reaches 69 682 USD compared to the reference cogeneration system. Consequently, the annual net revenue in the proposed cogeneration system (299 894 USD) is 28.94% higher than that in the reference cogeneration system (232 592 USD). The *PBP* of this proposed cogeneration system and the reference cogeneration system is 5.11 years and 6.50 years, respectively. The *TNPV* of the investigated systems varies with their operating times are presented in Fig. 7. Although the initial investment in this proposed cogeneration system is higher, the *TNPV* of this proposed cogeneration system exceeds that of the reference cogeneration system for no more than two years of operation. Then, the difference between the *TNPV* of the two investigated systems increases rapidly. The *TNPV* of the proposed and reference cogeneration systems at the end of their lifespans is 2 441 581 USD and 1 655 833 USD, respectively. A profit of 785 748 USD can be obtained by employing the proposed cogeneration system instead of the reference cogeneration system.

Table 9 Economic performances of the investigated systems

Items	Proposed cogeneration system	Reference cogeneration system
Initial investment/USD	1 326 596	1 267 099
ICE/USD	892 448	892 448
HRSG/USD	187 034	187 034
HACHP	104 979	–
Gas boiler/USD	–	51 856
Auxiliary equipment/USD	142 135	13 5761
Annual net revenue/USD·a^{-1}	299 894	232 592
Electricity/USD·a^{-1}	900 347	900 347
Steam/USD·a^{-1}	140 759	140 759
Fuel/USD·a^{-1}	–688 149	–757 830
O&M cost/USD·a^{-1}	–53 064	–50 684
TNPV/USD	2 441 581	1 655 833
PBP/a	5.11	6.50

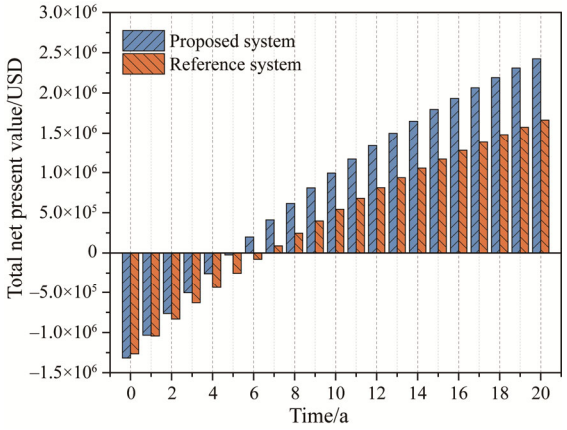

Fig. 7 The total net present value varies with the operation time

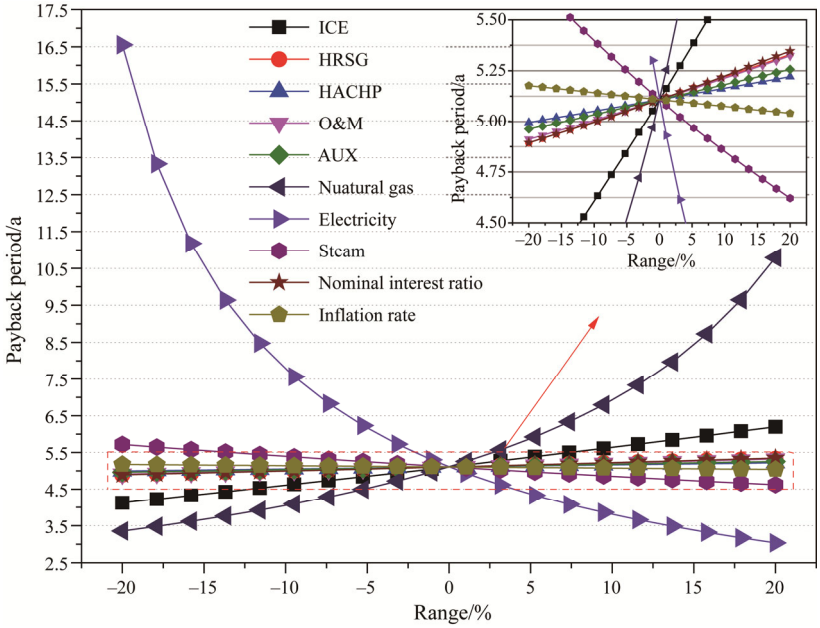

Fig. 8 The payback period varies with plant investment and revenue

The *PBP* of the proposed cogeneration system is determined under a series of fixed economic parameters and constant component costs; however, these parameters and costs are different from place to place and time to time in practice. It is important to reveal the effects of these parameters and costs on the *PBP* of the proposed cogeneration system, which can provide more useful information for investors. A variation of ±20% in these parameters and costs is selected to investigate their effects on the *PBP*, and the results are presented in Fig. 8. The variation of the *PBP* is less than one year for most of these investigated parameters, except for the ICE cost, the electricity price and the natural gas price. The results indicate that if the electricity price, the steam price and the inflation rate increase or if the ICE cost, the HRSG cost, the HACHP cost, the O&M cost, the AUX cost, the natural gas price and nominal interest ratio decrease, the *PBP* will be shortened and the proposed cogeneration system will be more attractive to investors. The price of electricity is the largest influencing factor, followed by the natural gas price, the ICE cost and the steam price, while the effects of other investigated parameters are insignificant (less than a half year). A price drop of electricity by 20% will directly make it take more than four-fifths of the lifespan of the proposed cogeneration system to recover its investment. In contrast, the investment of the proposed cogeneration system can be reclaimed in approximately three years when the electricity price increases to 0.144 USD/kWh (+20%). The *PBP* increases from 3.358 years to 10.79 years when the price of natural gas varies from 0.28 USD/m^3 to 0.42 USD/m^3 (–20% to +20%). The *PBP* varies between 4.125 years and 6.199 years when the variation of the ICE cost is less than 20% (varies between 713 958 USD and 1 070 938 USD). The *PBP* decreases to 4.621 years when the price of steam increases to 0.0156 USD/kg (+20%); by contrast, the value will increase to 5.718 years when the price of steam drops to 0.0104 USD/kg (–20%).

5. Conclusion

A high-temperature heat pump enhanced steam and power cogeneration system is proposed in this work. The effects of the heat pump on the thermodynamic, environmental protection, economic performances of the cogeneration system are identified. The low-temperature heat that cannot generate steam is recovered and upgraded by the heat pump to generate high-temperature process steam. Based on the simulation results, the energy can be used more efficiently, economically and cleanly in the proposed cogeneration system. The main conclusions obtained in this work are presented as follows:

(1) According to the energy analysis, the primary energy ratio and the energy saving ratio in the proposed cogeneration system reach 72.52% and 22.01%, which are 10.13% and 55.98% higher than those in the reference cogeneration system without heat pump, respectively.

(2) The proposed cogeneration system has better environmental performance. A CO_2 and NO_x emission reduction of 9.19% can be obtained compared to the system without the heat pump, which means approximately 372.64 tons of CO_2 and 3.02 tons of NO_x

emission can be avoided per year.

(3) The exergy efficiency of the proposed cogeneration system (46.28%) increases by 10.13% compared to that of the system without the heat pump. The exergy destruction in each component of the HACHP subsystem is no more than 1.2% owing to the cascade utilization of the HRSG flue gas and the jacket water residual energies.

(4) The payback period of this proposed cogeneration system is 5.11 years, which is 21.38% shorter than that of the system without low-temperature heat recovery. The total net present value of this proposed cogeneration system at the end of its lifespans is 2 441 581 USD and a profit of 785 748 USD can be obtained by employing the proposed cogeneration system instead of the reference cogeneration system. Natural gas and electricity prices are the determining factors affecting the payback period.

Acknowledgements

This work was supported by the National Key Research and Development Program of China (No. 2016YFF0201503).

References

[1] Birol F., World Energy Balances, in, International Energy Agency, International Energy Agency, 2019.

[2] Deymi-Dashtebayaz M., Tayyeban E., Multi objective optimization of using the surplus low pressure steam from natural gas refinery in the thermal desalination process, Journal of Cleaner Production, 2019, 238: 117945.

[3] De Corato U., Cancellara F.A., Measures, technologies, and incentives for cleaning the minimally processed fruits and vegetables supply chain in the Italian food industry, Journal of Cleaner Production, 2019, 237: 117735.

[4] Tumen Ozdil N.F., Tantekin A., Erbay Z., Energy and exergy analyses of a fluidized bed coal combustor steam plant in textile industry, Fuel, 2016, 183: 441–448.

[5] Hasanbeigi A., Harrell G., Schreck B., Monga P., Moving beyond equipment and to systems optimization: techno-economic analysis of energy efficiency potentials in industrial steam systems in China, Journal of Cleaner Production, 2016, 120: 53–63.

[6] Yang M., Dixon R.K., Investing in efficient industrial boiler systems in China and Vietnam, Energy Policy, 2012, 40: 432–437.

[7] Giaccone L., Canova A., Economical comparison of CHP systems for industrial user with large steam demand, Applied Energy, 2009, 86: 904–914.

[8] Jradi M., Riffat S., Tri-generation systems: Energy policies, prime movers, cooling technologies, configurations and operation strategies, Renewable and Sustainable Energy Reviews, 2014, 32: 396–415.

[9] Wang J, Wu J. Investigation of a mixed effect absorption chiller powered by jacket water and exhaust gas waste heat of internal combustion engine. International Journal of Refrigeration. 2015, 50: 193–206.

[10] Liu F.G., Tian Z.Y., Ma Z.X., Jia L.L., Zhang R., Yan A.-B., Experimental research on the property of water source gas engine-driven heat pump system with chilled and hot water in summer, Applied Thermal Engineering, 2020, 165: 114532.

[11] Aly W.I.A., Abdo M., Bedair G., Hassaneen A.E., Thermal performance of a diffusion absorption refrigeration system driven by waste heat from diesel engine exhaust gases, Applied Thermal Engineering, 2017, 114: 621–630.

[12] Chatzopoulou M.A., Markides C.N., Thermodynamic optimisation of a high-electrical efficiency integrated internal combustion engine – Organic Rankine cycle combined heat and power system, Applied Energy, 2018, 226: 1229–1251.

[13] Yang K., Zhu N., Ding Y., Chang C., Wang D., Yuan T., Exergy and exergoeconomic analyses of a combined cooling, heating, and power (CCHP) system based on dual-fuel of biomass and natural gas, Journal of Cleaner Production, 2019, 206: 893–906.

[14] Javan S., Mohamadi V., Ahmadi P., Hanafizadeh P., Fluid selection optimization of a combined cooling, heating and power (CCHP) system for residential applications, Applied Thermal Engineering, 2016, 96: 26–38.

[15] Yan Y., Zhang H., Long Y., Wang Y., Liang Y., Song X., Yu J.J.Q., Multi-objective design optimization of combined cooling, heating and power system for cruise ship application, Journal of Cleaner Production, 2019, 233: 264–279.

[16] Pérez N.P., Machin E.B., Pedroso D.T., Roberts J.J., Antunes J.S., Silveira J.L., Biomass gasification for combined heat and power generation in the Cuban context: Energetic and economic analysis, Applied Thermal Engineering, 2015, 90: 1–12.

[17] Segurado R., Pereira S., Correia D., Costa M., Techno-economic analysis of a trigeneration system based on biomass gasification, Renewable and Sustainable Energy Reviews, 2019, 103: 501–514.

[18] Mohammadkhani F., Yari M., A 0D model for diesel engine simulation and employing a transcritical dual loop Organic Rankine Cycle (ORC) for waste heat recovery from its exhaust and coolant: Thermodynamic and economic analysis, Applied Thermal Engineering, 2019, 150: 329–347.

[19] Song X., Liu L., Zhu T., Zhang T., Wu Z., Comparative analysis on operation strategies of CCHP system with

cool thermal storage for a data center, Applied Thermal Engineering, 2016, 108: 680–688.

[20] Yu X., Zhang Y., Kong L., Zhang Y., Thermodynamic analysis and parameter estimation of a high-temperature industrial heat pump using a new binary mixture, Applied Thermal Engineering, 2018, 131: 715–723.

[21] Urbanucci L., Bruno J.C., Testi D., Thermodynamic and economic analysis of the integration of high-temperature heat pumps in trigeneration systems, Applied Energy, 2019, 238: 516–533.

[22] Jensen J.K., Reinholdt L., Markussen W.B., Elmegaard B., Investigation of ammonia/water hybrid absorption/compression heat pumps for heat supply temperatures above 100°C, in: International Sorption Heat Pump Conference, University of Maryland, Washington DC, 2014, 1055: 1–10.

[23] Liu C., Jiang Y., Han W., Kang Q., A high-temperature hybrid absorption-compression heat pump for waste heat recovery, Energy Conversion and Management, 2018, 172: 391–401.

[24] Misra R.D., Sahoo P.K., Gupta A., Thermoeconomic evaluation and optimization of an aqua-ammonia vapour-absorption refrigeration system, International Journal of Refrigeration, 2006, 29: 47–59.

[25] Ahrendts J., Reference states, Energy, 1980, 5: 666–677.

[26] Balli O., Aras H., Hepbasli A., Thermodynamic and thermoeconomic analyses of a trigeneration (TRIGEN) system with a gas–diesel engine: Part I – Methodology, Energy Conversion and Management, 2010, 51: 2252–2259.

[27] Abbasi M., Chahartaghi M., Hashemian S.M., Energy, exergy, and economic evaluations of a CCHP system by using the internal combustion engines and gas turbine as prime movers, Energy Conversion and Management, 2018, 173: 359–374.

[28] Silveira J.L., Tuna C.E., Thermoeconomic analysis method for optimization of combined heat and power systems. Part I, Progress in Energy and Combustion Science, 2003, 29: 479–485.

[29] Aminyavari M., Najafi B., Shirazi A., Rinaldi F., Exergetic, economic and environmental (3E) analyses, and multi-objective optimization of a CO_2/NH_3 cascade refrigeration system, Applied Thermal Engineering, 2014, 65: 42–50.

[30] Baghernejad A., Yaghoubi M., Exergoeconomic analysis and optimization of an Integrated Solar Combined Cycle System (ISCCS) using genetic algorithm, Energy Conversion and Management, 2011, 52: 2193–2203.

[31] Zare V., Mahmoudi S.M.S., Yari M., Amidpour M., Thermoeconomic analysis and optimization of an ammonia–water power/cooling cogeneration cycle, Energy, 2012, 47: 271–283.

[32] Su B., Han W., Jin H., An innovative solar-powered absorption refrigeration system combined with liquid desiccant dehumidification for cooling and water, Energy Conversion and Management, 2017, 153: 515–525.

[33] Su B., Han W., Chen Y., Wang Z., Qu W., Jin H., Performance optimization of a solar assisted CCHP based on biogas reforming, Energy Conversion and Management, 2018, 171: 604–617.

[34] Su B., Han W., Sui J., Jin H., A two-stage liquid desiccant dehumidification system by the cascade utilization of low-temperature heat for industrial applications, Applied Energy, 2017, 207: 643–653.

[35] Su B., Qu W., Han W., Jin H., Feasibility of a hybrid photovoltaic/thermal and liquid desiccant system for deep dehumidification, Energy Conversion and Management, 2018, 163: 457–467.

[36] Sanaye S., Meybodi M.A., Shokrollahi S., Selecting the prime movers and nominal powers in combined heat and power systems, Applied Thermal Engineering, 2008, 28: 1177–1188.

[37] Jiang R., Han W., Qin F.G.F., Sui J., Yin H., Yang M., Xu Y., Thermodynamic model development, experimental validation and performance analysis of a MW CCHP system integrated with dehumidification system, Energy Conversion and Management, 2018, 158: 176–185.

[38] Department of environment, food and rural affairs, 2013 Government GHG conversion factors for company reporting: Methodology paper for emission factors.

[39] Bengtsson S., Andersson K., Fridell E., A comparative life cycle assessment of marine fuels: liquefied natural gas and three other fossil fuels, Proceedings of the Institution of Mechanical Engineers, Part M: Journal of Engineering for the Maritime Environment, 2011, 225: 97–110.

[40] Klein S.A., Alvarado F., Engineering Equation Solver (EES), FChart Software, 2011.

Appendix A: Parameters and model of the primary mover

The ICE model developed by Sanaye et al. [36] is adopted to calculate the engine characteristics at various operating conditions, which has been verified to agree well with the experimental data of an ICE (with the type CAT G3512E) [37].

The fuel mass flow rate consumption at part load (*PL*):

$$m_{\mathrm{f}} = \left[-0.02836 \cdot \exp\left(-3.254 \cdot PL\right) + 0.2556 \cdot \exp\left(1.912 \cdot PL\right)\right] \cdot m_{\mathrm{ICE},0} \tag{A.1}$$

where *PL* is the part load of the ICE, which is in the range of 0 to 1. $m_{\mathrm{ICE},0}$ is the nominal fuel mass flow rate, m^3/h.

Then, the thermal energy input can be calculated by:

$$Q_{\mathrm{fuel}} = \frac{m_{\mathrm{f}} \cdot \mathrm{LHV_f}}{3600} \tag{A.2}$$

where LHV_{f} is the low calorific value of fuel, kJ/m^3.

The thermal efficiency at part load:

$$\eta_{\mathrm{ICE}} = \left[1.07 \cdot \exp\left(-0.05736 \cdot PL\right) - 1.259 \cdot \exp\left(-5.367 \cdot PL\right)\right] \cdot \eta_{\mathrm{ICE},0} \tag{A.3}$$

where $\eta_{\mathrm{ICE},0}$ represents the nominal efficiency of the ICE.

The electric power export of the ICE can be obtained by:

$$P_{\mathrm{ICE}} = \eta_{\mathrm{ICE}} \cdot Q_{\mathrm{fuel}} \tag{A.4}$$

The thermal energy could be recovered from jacket water and flue gas:

$$Q_{\mathrm{fg}} = \left(0.1016 \cdot PL^2 - 0.1423 \cdot PL + 0.3172\right) \cdot Q_{\mathrm{fuel}} \tag{A.5}$$

$$Q_{\mathrm{jw}} = \left[0.2401 \cdot \exp\left(-2.48 \cdot PL\right) + 0.1535 \cdot \exp\left(0.2822 \cdot PL\right)\right] \cdot Q_{\mathrm{fuel}} \tag{A.6}$$

Then, the heat loss of the ICE can be obtained according to the energy balance:

$$Q_{\mathrm{loss}} = Q_{\mathrm{fuel}} - Q_{\mathrm{fg}} - Q_{\mathrm{jw}} - P_{\mathrm{ICE}} \tag{A.7}$$

The flue gas temperature at the ICE outlet under part load conditions is calculated as follows based on the actual operating data of the ICE CAT G3512E.

$$T_{\mathrm{fg}} = 658.66 - 334.06 \cdot PL + 109.48 \cdot PL^2 \tag{A.8}$$